Light scattering by liquid LiCl: a computer simulation and theoretical study

1990 J. Phys.: Condens. Matter 2 SA257

(http://iopscience.iop.org/0953-8984/2/S/038)

J. Phys.: Condens. Matter 2 (1990) SA257–SA263. Printed in the UK

Light scattering by liquid LiCl: a computer simulation and theoretical study

P A Madden† and K O'Sullivan‡

† Department of Physical Chemistry, Oxford University, South Parks Road, Oxford OX1 3QZ, UK

‡ Department of Theoretical Physics, Oxford University, Keble Road, Oxford OX1 3NP, UK

Received 6 August 1990

Abstract. The physical processes responsible for the 'interaction-induced' polarizabilities in ionic melts are investigated by electronic structure calculations. These are built into a computationally tractable model for the polarizability of the melt whose correlation functions are then calculated by molecular dynamics simulation. The experimental light scattering data are quantitatively reproduced. A theory of the lineshape is verified with the simulation data. The influences on the lineshape of the various dynamical modes of the ionic system (e.g. the plasmon mode) are thereby assessed.

1. Introduction

Raman (or Rayleigh-wing) light scattering by simple ionic materials has been studied experimentally for many years (Clarke and Woodcock 1972, Giergiel *et al* 1984, Bunten *et al* 1986, McGreevy 1987). The scattering is caused by the fluctuations in the polarizability density of the melt induced by the inter-ionic interactions; as such it belongs to the general class of 'interaction-induced' spectroscopic phenomena (Birnbaum 1985). These phenomena have been extensively investigated in van der Waals (molecular) materials and considerable insight into the intermolecular dynamics has been obtained therefrom. In contrast, in ionic materials the mechanisms responsible for the interaction-induced polarizability are not understood even semi-quantitatively and consequently the dynamical processes which determine the lineshape have not been identified.

This work, then, has two objectives. Firstly to characterise the interaction-induced polarizability and to express its dependence on the inter-ionic positions in a computationally tractable form. Other, non-spectroscopic properties of ionic materials also depend on the way the polarizability of an ion is influenced by the positions of its neighbours. An example is the induction (or polarization) energy of an ion at a defect or interface in a crystal. Thus the development of a polarizability model capable of reproducing the light scattering spectrum should also be useful in building potential models for ionic materials. The second objective is to use this polarizability model to understand which dynamical processes in the melt are responsible for the characteristic shape of the spectrum. Since the shape reflects the time dependence of the inter-ionic positions, i.e. the structural relaxation, it is possible that the spectrum could be used

0953-8984/90/SA0257+07$03.50

to study dynamical events in ionic melts not observable by other means. All of the results described in this paper relate to lithium chloride; this work forms part of a more general survey of light scattering in the alkali halides (O'Sullivan 1990).

2. Fluctuating polarizability and light scattering in ionic melts

The light scattering spectrum is related to the spectrum of the fluctuations in the total polarizability $\Delta\boldsymbol{\Pi}$ of the sample. For an isotropic fluid, there are two independent spectra which are given by the fluctuations in the isotropic and anisotropic parts of the tensor $\Delta\boldsymbol{\Pi}$; i.e.

$$I^{\mathrm{ISO}}(\omega) = G_{\mathrm{c}} \int_0^\infty \mathrm{e}^{-\mathrm{i}\omega t} \langle (\Delta\boldsymbol{\Pi}_{\mathrm{ISO}}(0)) \cdot (\Delta\boldsymbol{\Pi}_{\mathrm{ISO}}(t)) \rangle \tag{1}$$

and

$$I^{\mathrm{ANI}}(\omega) = G_{\mathrm{c}} \int_0^\infty \mathrm{e}^{-\mathrm{i}\omega t} \langle (\Delta\boldsymbol{\Pi}_{\mathrm{ANI}}(0)) \cdot (\Delta\boldsymbol{\Pi}_{\mathrm{ANI}}(t)) \rangle \tag{2}$$

where G_{c} is a known geometrical factor. The isotropic part of the tensor is simply the trace,

$$\boldsymbol{\Pi}_{\mathrm{ISO}} = \tfrac{1}{3}\mathrm{Tr}\ \boldsymbol{\Pi} \tag{3}$$

and the anisotropic part of the tensor may be expressed by any of five representations whose correlation functions behave identically, e.g.

$$\boldsymbol{\Pi}_{\mathrm{ANI}} = 2\Pi_{zz} - \Pi_{xx} - \Pi_{yy}. \tag{4}$$

The experimentally determined polarised and depolarised spectra are given by:

$$I^{\mathrm{POL}}(\omega) = I^{\mathrm{ISO}}(\omega) + \tfrac{4}{3} I^{\mathrm{ANI}}(\omega) \tag{5}$$

and,

$$I^{\mathrm{DEPOL}}(\omega) = I^{\mathrm{ANI}}(\omega) \tag{6}$$

and the depolarization ratio is:

$$\rho(\omega) = \frac{I^{\mathrm{DEPOL}}(\omega)}{I^{\mathrm{POL}}(\omega)}. \tag{7}$$

This can be seen to have a maximum value of 0.75 when there is no isotropic scattering.

The first objective, of finding a model for the fluctuating polarizability, has been pursued via *ab initio* electronic structure calculations and computer simulation studies of the melt. The simulated spectra, from the above expresions, are then compared with experiment. It may be anticipated that several physically distinct processes may contribute to the fluctuations, distortion of the ion by the Coulomb fields of the other ions and by short-range overlap interactions and the dipole-induced dipole (DID) processes, which are the dominant source of the interaction-induced spectra of van der

Waals materials (Birnbaum 1985). As discussed extensively elsewhere (Madden and Board 1987), these contributions may be expressed through:

$$\Delta\boldsymbol{\Pi}(t) = \boldsymbol{\Pi}^{\mathrm{DID}}(t) + \boldsymbol{\Pi}^{\mathrm{SR}}(t) + \boldsymbol{\Pi}^{\mathrm{B}}(t) + \boldsymbol{\Pi}^{\gamma}(t) \; . \tag{8}$$

The individual contributions have been examined quantitatively in *ab initio* studies of distorted crytals (Fowler and Madden 1985). $\boldsymbol{\Pi}^{\mathrm{B}}$ and $\boldsymbol{\Pi}^{\gamma}$ give the changes in the anion polarizabilities induced by the Coulomb field gradient and field respectively, the corresponding changes in cation polarizabilities are negligible. They are given by:

$$\Pi^{\gamma}_{\alpha\beta} = \sum_i \tfrac{1}{2}\gamma^i \left(\sum_j q_j \nabla_\alpha r_{ij}^{-1} \right) \left(\sum_k q_k \nabla_\beta r_{ik}^{-1} \right) \tag{9}$$

and,

$$\Pi^{\mathrm{B}}_{\alpha\beta} = \sum_i \tfrac{1}{3} B^i \sum_j q_j \nabla_\alpha \nabla_\beta r_{ij}^{-1} . \tag{10}$$

where γ^i and B^i are hyperpolarizabilities (Fowler and Madden 1984a, b), which are taken as zero for cations.

$\boldsymbol{\Pi}^{\mathrm{SR}}$ is the short-range or 'dent-in-the-wall' (Fowler and Madden 1985) contribution from the distortion of the anions, again the cation contributions are negligible. Madden and Board (1987) proposed that this process, which reflects the distortion of the local coordination shell around an ion in the melt, could be represented in a computationally tractable way via a modified Drude model in which the polarizability of an ion is written as

$$\alpha^i = \; q\boldsymbol{K}_i^{-1} \tag{11}$$

where q is a charge bound on a spring whose force constant $\boldsymbol{K}_i$ is a second-rank symmetric tensor—to reflect the non-isotropic nature of the instantaneous environment of ion i. It is expressed as a function of the instantaneous pair separations to facilitate the computation. The most general expression of this form is

$$\boldsymbol{K}_i(\boldsymbol{R}^N) = \left(K^0 + \sum_{j\neq i} A(r_{ij}) \right) \cdot \boldsymbol{I} + \sum_{j\neq i} B(r_{ij})(3\hat{\boldsymbol{r}}_{ij} \cdot \hat{\boldsymbol{r}}_{ij} - \boldsymbol{I}). \tag{12}$$

The functions $A(r_{ij})$ and $B(r_{ij})$ represent the effects on the Drude force constant of the short-range inter-ionic interactions. If these are zero, then we recover the free ion value for $\boldsymbol{K}$, namely K_0. We note in passing that any off-diagonal contributions to $\boldsymbol{K}$ will arise from the function $B(r_{ij})$, and thus this function describes the anisotropic contributions to α^i. Likewise, the function $A(r_{ij})$ will contain any isotropic changes in the short-range part of the polarizability tensor. The forms chosen for $A(r_{ij})$ and $B(r_{ij})$ were similar to the Born–Mayer part of the short-range inter-ionic potential:

$$A(r_{ij}) = a_{ij} \exp(-c_{ij}(r_{ij} - \sigma_{ij})) \tag{13}$$

$$\mathrm{B}(r_{ij}) = b_{ij} \exp(-d_{ij}(r_{ij} - \sigma_{ij})) \tag{14}$$

where the σ_{ij} are chosen to be the Fumi–Tosi ionic radii (Tosi and Fumi 1964). The values for the parameters a, b and c have been determined from the *ab initio* calculated values of α^{SR} for three different distortions of the nearest neighbour shell (Fowler and Madden 1985 and unpublished).

The remaining contribution to the total polarizability, in equation (8), is the first-order DID term:

$$\Pi^{DID}_{\alpha\beta} = \sum_i \alpha^i \sum_j \alpha^j \nabla_\alpha \nabla_\beta r_{ij}^{-1}. \tag{15}$$

where α^i is the ionic polarizability in the undistorted crystal environment. Note that $\boldsymbol{\Pi}^{DID}$ and $\boldsymbol{\Pi}^{B}$ can only contribute to the anisotropic spectrum, by virtue of Laplace's theorem.

3. Computer simulation of the light scattering spectra

Equations (8)–(15) provide explicit expresssions for the dependence of the polarizability of the system on the positions of the ions therein. Consequently the correlation functions which determine the spectra (equations (1)–(7)) can be calculated in a molecular dynamics computer simulation. We have performed such calculations using a rigid ion model (RIM) of the inter-ionic interactions, using Born–Mayer potential functions with the Fumi–Tosi parameters for LiCl (Rovere and Tosi 1986). The electric fields and field gradients and the DID tensor were calculated by an Ewald summation. The parameters of the polarizability model for LiCl are $\alpha^{Cl} = 6.18$, $\alpha^{Li} = 0.192$, $\gamma^{Cl} = 2270$, $B^{Cl} = -342$, $K^0 = 0.0335$, $a_{+-} = 0.0031$, $a_{--} = 0.0011$, $b_{+-} = 0.00275$, $b_{--} = 0.0011$, $c_{+-} = 0.400$, $c_{--} = 0.295$, $d_{+-} = 0.4425$ and $d_{--} = 0.2915$, where all values are in atomic units.

The isotropic and anisotropic spectra calculated in this way are compared with the experimental data of Giergiel *et al* (1984) in figures 1 and 2. The absolute intensities of the experimental spectra are not known and so the comparison is made by normalising the spectra at low frequency. The relative intensities of the isotropic and anisotropic spectra (i.e. the depolarization ratio) is predicted very well by the simulation, a value of 0.22 is found at zero frequency and the shape of $\rho(\omega)$ also agrees with experiment. The absolute intensity calculated for NaCl, using similar methods, agrees very well with experiment (Madden and Board 1987). The mean polarizability of the ions in the simulation may be used to predict the refractive index of the melt (Tessman *et al* 1953), the agreement with experiment is almost perfect.

The agreement between the calculated and experimental isotropic spectra is excellent, it extends over 500 cm^{-1} in frequency and nearly three decades of intensity. The simulation shows that the isotropic spectrum is dominated by the short-range mechanism for the polarizability fluctuations and therefore its shape reflects the relaxation of the first coordination shell around the anions.

The agreement of the anisotropic spectra is also good, it is found that $\boldsymbol{\Pi}^{DID}$, $\boldsymbol{\Pi}^{SR}$ and $\boldsymbol{\Pi}^{B}$ all make large contributions to this spectrum and that there is significant cross-correlation between them. Significant discrepancies between the simulated and experimental spectra arise in the $350 - 500$ cm^{-1} range. It appears that the shoulder which is prominent in the simulated spectrum at 470 cm^{-1} is more spread out in the experimental spectrum and occurs at lower frequency. Further work (see below)

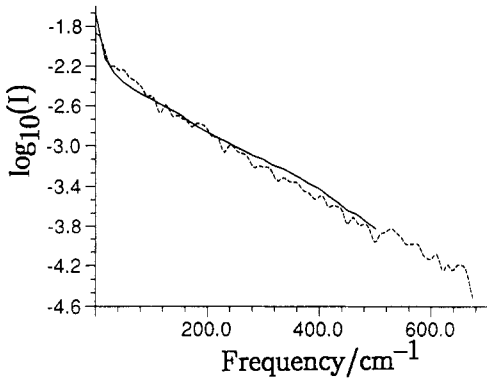

Figure 1. The Isotropic spectrum of molten LiCl: experiment, full curve (Giergiel *et al* 1984); simulation, broken curve.

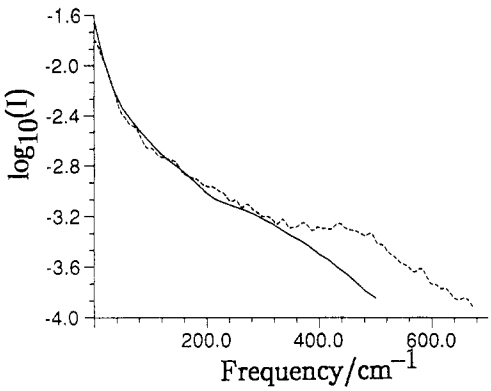

Figure 2. The Anisotropic spectrum of molten LiCl: experiment, full curve (Giergiel *et al* 1984); simulation, broken curve.

has suggested that the shoulder is caused by the plasmon, or charge density wave, oscillation mode of the fluid. The reasons for the discrepancy can therefore be traced to our use of a rigid-ion model. Since this model ignores the effect of electronic polarization on the ionic dynamics it is to be expected that the plasmon mode of the simulated fluid will occur at too high a frequency and be less damped than in reality (Rovere and Tosi 1986). We have directly checked this hypothesis by calculating the light scattering spectra with a shell model for the inter-ionic interactions; electronic polarization effects are included in this model. The simulated anisotropic spectra using the shell model are in excellent agreement with experiment (O'Sullivan 1990).

4. Ionic dynamics and the light scattering spectra

The agreement of the calculated and experimental spectra suggests that the polarizability model is a good one and thus that we can now claim to know the functional form for the dependence of the interaction-induced polarizability on ionic positions. It therefore becomes possible to examine the fluctuating polarizability correlation functions theoretically and see how the dynamical modes of the melt influence the lineshape. Of particular interest is the role of the plasmon mode, associated with the

oscillations of the Fourier components of the charge density (Hansen and McDonald 1986). This mode has proven difficult to study experimentally.

The link between the spectra of the components of the fluctuating polarizability, $\mathbf{\Pi}^{SR}$, $\mathbf{\Pi}^{B}$, etc, and the local density fluctuations in the fluid can be developed in close analogy with the theory of the DID spectrum of an atomic fluid (Madden 1978). Here we restrict attention to $\mathbf{\Pi}^{B}$ terms, for which it can be shown (using the large difference between the masses of the Li and Cl ions) that (O'Sullivan 1990)

$$I^{B}(\omega) \propto \int \mathrm{d}t\ \mathrm{e}^{-\mathrm{i}\omega t} \int \mathbf{d}\boldsymbol{k} \int \mathbf{d}\boldsymbol{k}' f(\boldsymbol{k}) f(\boldsymbol{k}') \langle (\rho_m(-\boldsymbol{k})\rho_q(\boldsymbol{k}))(t) \cdot (\rho_m(\boldsymbol{k}')\rho_q(\boldsymbol{k}'))(0) \rangle \quad (16)$$

where $f(\boldsymbol{k})$ is the spatial Fourier transform of the dipole tensor $\nabla_\alpha \nabla_\beta r^{-1}$ and $\rho_m(\boldsymbol{k})$ and $\rho_q(\boldsymbol{k})$ are the spatial Fourier components of the mass and charge density of the melt, respectively. Following Madden (1978), the correlation function in (16) is factorised using the standard mode-coupling approximation; translational invariance allows us to ignore terms with $\boldsymbol{k} \neq \boldsymbol{k}'$ and then the only surviving terms in the correlation function are

$$I^{B}(\omega) \propto \int \mathrm{d}t\ \mathrm{e}^{-\mathrm{i}\omega t} \int \mathrm{d}k\ k^2 f^2(k) \langle \rho_m(-k,t)\rho_m(k,0) \rangle \langle \rho_q(k,t)\rho_q(-k,0) \rangle. \quad (17)$$

The two correlation functions are just the mass- and charge-weighted intermediate scattering functions, $F_{MM}(k,t)$ and $F_{QQ}(k,t)$, which may, in principle, be studied by inelastic neutron scattering (Hansen and McDonald 1986). In the hydrodynamic regime of low k, the former has a spectrum which shows a central (Rayleigh) line and two shifted sound or Brillouin peaks, whereas the latter has a spectrum consisting of a central diffusive peak and the shifted plasmon oscillation, the propogating modes disappear at higher values of k in a way which is not well characterised (Hansen and McDonald 1986). At very high k values both functions become free-particle-like. Equation (17) shows how these well known features may enter into the light scattering spectrum. The equation may be rewritten as:

$$I^{B}(\omega) \propto \int \mathrm{d}t\ \mathrm{e}^{-\mathrm{i}\omega t} \int \mathrm{d}k\ k^2 f^2(k) S_{MM}(k) S_{QQ}(k) C_{MMQQ}(k,\omega) \quad (18)$$

where $S_{MM}(k)$ and $S_{QQ}(k)$ are the mass and charge structure factors and

$$C_{MMQQ}(k,\omega) = \int \mathrm{d}t\ \mathrm{e}^{-\mathrm{i}\omega t} F_{MM}(k,t) F_{QQ}(k,t) / S_{MM}(k) S_{QQ}(k). \quad (19)$$

This gives us an approximate expression for the spectra in terms of a dynamical function $C_{MMQQ}(k,\omega)$, weighted by the k-dependent function $k^2 f^2(k) S_{MM}(k) S_{QQ}(k)$.

We have examined the validity of this expression for the spectrum by calculating the mass and charge intermediate scattering functions at several values of k between the lowest accessible value and an upper limit of 9.3 $\mathrm{\AA}^{-1}$, this covers the range in which the weighting function is non-zero. The spectra of the calculated functions conform to expectations; the plasmon peak in the spectrum of $F_{QQ}(k,t)$ occurs at a frequency of about 470 cm^{-1}. This peak is also found in $C_{MMQQ}(k,\omega)$, it persists up to k values of about 2/3 of that of the principal peak of $S_{MM}(k)$.

In figure 3 we show the comparison of the spectrum predicted by the theory, using the $C_{MMQQ}(k,\omega)$ calculated in the simulation and an appropriate weight function,

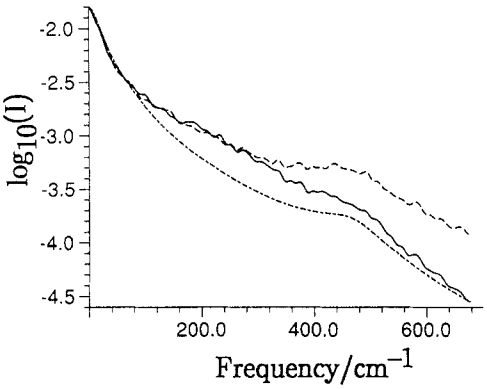

Figure 3. Comparison of the spectrum of Π^B, calculated in the simulation (full curve), with that calculated from the theoretical expression in equation (17) (chain curve). The total spectrum is shown for comparison (broken curve).

with the B-term simulated spectrum and also the total simulated depolarised spectrum, all on a logarithmic intensity scale. The spectrum predicted by equations (4.10)–(15) is seen to agree remarkably well with the B-term spectrum and also to exhibit the spectral features apparent in the total spectrum. The agreement is closest in the low-frequency region $0 \rightarrow 100$ cm^{-1}, where the sharp drop in intensity is well reproduced. This allows us to identify the low-frequency drop-off feature with fluctuations in the mass and charge density at k-values close to the principal peak in $S(k)$. Also apparent in the predicted spectra is the shoulder at about 470 cm^{-1}, which may therefore be unambiguously identified as the signature of the plasmon mode in the melt, associated with hydrodynamic charge density fluctuations at values of k below the first peak of $S(k)$.

On the basis of these investigations, we may now assign the low-frequency drop-off feature in the spectrum to mass and charge density fluctuations at wavelengths characteristically close to to the principal peak of the structure factor. The shoulder feature is assigned to the hydrodynamic charge density fluctuations at values of k below the first peak of $S(k)$.

References

Birnbaum G (ed) 1985 *Phenomena Induced by Intermolecular Interactions* (New York: Plenum)
Bunten R A J, McGreevy R L, Mitchell E W J and Raptis C 1986 *J. Phys. C: Solid State Phys.* **19** 2925
Clarke J H R and Woodcock L V 1972 *J. Chem. Phys.* **57** 1006
Fowler P W and Madden P A 1984a *Phys. Rev.* B **29** 1035
—— 1984b *Phys. Rev.* B **30** 6131
—— 1985 *Phys. Rev.* B **31** 5443
Giergiel G, Subbaswamy K R and Eklund P C 1984 *Phys. Rev.* B **29** 3490
Hansen J P and McDonald I R 1986 *Theory of Simple Liquids* (London: Academic)
Madden P A 1978 *Mol. Phys.* **36** 365–88
Madden P A and Board J A 1987 *J. Chem. Soc. Faraday Trans.* 2 **83** 1891
McGreevy R L 1987 *J. Chem. Soc. Faraday Trans.* 2 **83** 1875
O'Sullivan K 1990 *DPhil Thesis* University of Oxford
Rovere M and Tosi M P 1986 *Rep. Prog. Phys.* **49** 1001
Tessman J R, Kahn A H and Shockley W 1953 *Phys. Rev.* **92** 890
Tosi M P and Fumi F G 1964 *J. Phys. Chem. Solids* **25** 31–45